Unconstrained Parametrization of Dissipative and Contracting Neural Ordinary Differential Equations

Daniele Martinelli, Clara Lucía Galimberti, Ian R. Manchester, Luca Furieri, and Giancarlo Ferrari-Trecate

***Abstract*— In this work, we introduce and study a class of Deep Neural Networks (DNNs) in continuous-time. The proposed architecture stems from the combination of Neural Ordinary Differential Equations (Neural ODEs) with the model structure of recently introduced Recurrent Equilibrium Networks (RENs). We show how to endow our proposed NodeRENs with contractivity and dissipativity — crucial properties for robust learning and control. Most importantly, as for RENs, we derive parametrizations of contractive and dissipative NodeRENs which are unconstrained, hence enabling their learning. We also show that these parametrizations can be less conservative than the corresponding ones for RENs. We validate the properties of NodeRENs, including the possibility of handling irregularly sampled data, on a case study on nonlinear system identification.**

I. Introduction

Learning complex nonlinear mappings from data is a fundamental task in many engineering applications, including computer vision, healthcare, internet of things, and smart cities [1]. Deep Neural Networks (DNNs) have emerged as an effective tool to deal with these tasks, thanks to their flexibility and ability to generalize their predictions based on massive amounts of data. Despite their effectiveness, DNNs tend to lack robustness: a slight change in the input data may yield highly different outputs, eventually leading to poor generalization capabilities [2]–[5]. Such behavior is especially problematic when DNNs are implemented in physical systems, such as safety-critical power grids or robots that interact with humans. In these applications, sensor measurements are inevitably affected by multiple sources of noise and uncertainty, and a lack of robustness may result in significant losses.

In order to endow DNN models with formal stability and robustness guarantees, [4] proposes equipping DNN layers with a dynamical system interpretation. The work [6] establishes dynamical DNN models which universally approximate all nonlinear dynamical systems defined in discrete-time and proposes a set of convex constraints that enforce stability of the DNN model during training. In [7], the authors have developed discrete-time Recurrent Equilibrium Networks (RENs) that result from the closed-loop interconnection of a discrete-time linear dynamical system with a static nonlinearity. A main contribution of [7] is to provide an unconstrained parametrization (also known as *direct* parametrization) of a class of RENs with properties of stability and dissipativity that are *built-in*, i.e., that hold for any choice of the parameters, and without the need to constrain them to a subset. This property enables parameter optimization for very deep models through unconstrained-gradient-descent-based algorithms, while ensuring stability and dissipativity at any iteration.

The usefulness of RENs for system identification and optimal control has been demonstrated in [7] and [8], respectively. However, the corresponding stability and dissipative guarantees are only compatible with discrete-time or sampled-data systems. Studying how the properties of nonlinear discrete-time dynamics port to their continuous-time counterpart is usually a challenging problem [9].

The recently proposed Neural Ordinary Differential Equations (Neural ODEs) [10] bridge the concepts of DNNs and continuous-time dynamics. Specifically, the authors of [10] suggest unfolding infinitely many DNN layers as specified by a parametrized ODE, and training the network by using the adjoint sensitivity method [11]. Neural ODEs enjoy several benefits over discrete DNN models such as [4], [6], [7], including memory savings, adaptive computations beyond Euler-like integration methods, and the ability to include data that arrive at arbitrary instants in the time continuum. Starting from Neural ODEs, in [12], the authors proposed a continuous-time analogous of Recurrent Neural Networks, although without guarantees of stability or dissipativity. The work [13] has proposed stable Hamiltonian Neural ODEs which further exhibit non-vanishing gradient flows. A class of Hamiltonian ODEs that further enjoy contractivity has been developed in [5]. Furthermore, while [14] derives architectures with guaranteed convergence of the flow to some stable set. However, an architecture that combines the strong stability, robustness, and expressivity properties of [6], [7] with the benefits of Neural ODEs is not available to the best of our knowledge.

A. Contributions

In this paper, we establish an alternative version of the REN architecture of [7] that is compatible with Neural ODEs in continuous-time. We accordingly denominate our architectures as *NodeRENs*. After showing that NodeRENs induce well-posed dynamical systems in continuous-time, we establish that our models enjoy stability and dissipativity properties by design, i.e., without any constraints on

D. Martinelli, C. L. Galimberti, L. Furieri and G. Ferrari-Trecate are with the Institute of Mechanical Engineering, EPFL, Switzerland. E-mail addresses: {daniele.martinelli, clara.galimberti, luca.furieri, giancarlo.ferraritrecate}@epfl.ch.

Ian Manchester is with the Australian Centre for Robotics (ACFR) and the School of Aerospace, Mechanical and Mechatronic Engineering, University of Sydney, Australia. E-mail address: ian.manchester@sydney.edu.au.

Research supported by the Swiss National Science Foundation (SNSF) under the NCCR Automation (grant agreement 51NF40_80545). Luca Furieri is also grateful to the SNSF for the Ambizione grant PZ00P2_208951.

the space of the parameters that describe the DNNs — akin to their discrete-time counterpart of [7]. At the same time, NodeRENs inherit the advantages of Neural ODEs in continuous-time; they are compatible with any integration scheme that can be chosen based on a trade-off between accuracy and resources, and they can be evaluated at any chosen time instant, without the requirement to be uniformly sampled in time.

The paper is structured as follows. In Section II, we provide a description of the problem setting, along with the definition of contractivity and Integral Quadratic Constraints (IQCs). In Section III, the NodeREN model is introduced. We present the steps to obtain NodeRENs that are contracting and dissipative by design. Moreover, in Section IV the NodeRENs are validated in continuous-time applications, on a nonlinear system identification problem. Finally, Section V summarizes the conclusions of this work and suggests future developments. Additionally, in the Appendix of our Technical Note [15], we report examples of NodeRENs used for binary classifications and as controllers for a multi-agent system.

B. Notation

We denote the set of real numbers as $\mathbb{R}$ and the set of non-negative real numbers as $\mathbb{R}_0^+$. For $T > 0$, let $PC([0,T],\mathbb{R}^n)$ be the space of piecewise-continuous functions in the time interval $[0,T]$. We represent the Euclidean norm of $v \in \mathbb{R}^n$ with $|v|$. For a square matrix X, we use the notation $X \succ 0$ ($X \succeq 0$) and $X \prec 0$ ($X \preceq 0$) to denote positive (semi-) definiteness and negative (semi-) definiteness, respectively. The minimum and maximum eigenvalues of the square matrix X are denoted as $\lambda_{min}(X)$ and $\lambda_{max}(X)$, respectively. We use $(*)$ to represent a symmetric term in a quadratic expression, e.g., $(X+Y)Q(*)^\top = (X+Y)Q(X+Y)^\top$, for some $Q \in \mathbb{R}^{n\times n}$ and $X, Y \in \mathbb{R}^{q\times n}$. With $(*)$, we also indicate elements in symmetric matrices that can be obtained by symmetry. We use $[M]_{p\times m}$ to indicate the block matrix with the first p rows and m columns of $M \in \mathbb{R}^{n\times n}$ with $n \geq m$ and $n \geq p$.

II. Problem Formulation

Consider a nonlinear system Σ_θ in continuous-time

$$\Sigma_\theta \;=\; \begin{cases} \dot{x}(t) = f_\theta(x(t), u(t)) \\ y(t) = g_\theta(x(t), u(t)) \end{cases}, \tag{1}$$

where $x(t) \in \mathbb{R}^n$, $y(t) \in \mathbb{R}^p$ and $u(t) \in \mathbb{R}^m$ denote the state, output and input of the system at any time $t \in \mathbb{R}_0^+$, respectively, and $x(0) = x_0$. In (1), $\theta \in \mathbb{R}^{n_\theta}$ denotes a vector of parameters affecting the behavior of the system. The idea behind Neural ODEs [10] is to interpret some specific DNNs (e.g., ResNets [16]) as discretized ODEs. Then, the family of Neural ODEs can be obtained when the discretization step converges to zero, effectively passing from discrete-time DNNs to continuous-time models as (1).[1] Accordingly, in this paper we consider the following learning problem:

$$\begin{aligned} \min_{\theta} \quad & L(\theta, \tilde{\mathcal{Z}}) \\ \text{subject to} \;\; & (1)\,. \end{aligned} \tag{2}$$

L is a scalar loss function that can depend on the trajectories $x(t)$ and $y(t)$ of (1), for $t \in [0,T]$ with $T > 0$, and $\tilde{\mathcal{Z}}$ is a given training data-set. For instance, in a classification task, $y(T)$ can play the role of the DNN output layer which is compared to the label y^j_{label} of the point $x^j(0)$ contained in a data-set $\tilde{\mathcal{Z}} = \left\{(x^j(0), y^j_{label})\right\}_{j=1}^N$ for $N \in \mathbb{N}$. Neural ODEs can exploit any chosen numerical method to perform the forward propagation and the gradient computations through (1), including those based on adaptive sampling in order to guarantee a desired level of precision (e.g., Dormand-Prince, Bogacki–Shampine [17]). Although possible, back-propagating through numerical solver's operations can be highly expensive in terms of memory and introduce numerical errors. As an alternative, to solve (2) one can use the adjoint method — we refer to [10] for full details.

Neural-ODEs in their general form are not guaranteed to yield stable or dissipative dynamical flows. Such properties are fundamental in optimal control and system identification, as well as in robust learning problems dealing with noisy features [5] and adversarial attacks [18]. Specifically, motivated by [7], in this paper, we focus on continuous-time systems that are contracting, and systems that satisfy incremental IQCs. We proceed with formally defining both.

Firstly, given a system Σ_θ with initial condition $a \in \mathbb{R}^n$ and an input function $u^{[1]} \in PC([0,\infty],\mathbb{R}^m)$, let $x_a^{[1]}$ and $y_a^{[1]}$ denote the corresponding state and output trajectories, respectively.

Definition 1. A system Σ_θ in the form (1) is said to be *contracting* if for any two initial conditions $a, b \in \mathbb{R}^n$ and given the same input trajectory $u^{[1]} \in PC([0,\infty],\mathbb{R}^m)$, the corresponding state trajectories $x_a^{[1]}$ and $x_b^{[1]}$ satisfy:

$$|x_a^{[1]}(t) - x_b^{[1]}(t)| \leq \kappa e^{-ct}|a-b|\,, \tag{3}$$

for all $t \in \mathbb{R}_0^+$ and for some $c > 0$, $\kappa > 0$.

The Definition 1 can be interpreted as follows: a contracting system 'forgets' the initial condition exponentially fast as time progresses. Hence, all trajectories converge to each other, independently of the initial state.

Next, we define dissipative systems that satisfy incremental IQCs. Dissipative systems cannot increase their internal energy despite external inputs (e.g., feedback control actions or disturbances). As such, they can be designed to possess finite input-output gains, a crucial property in nonlinear control theory [19], as well as robust learning [20]. In order to formally define these properties, let $a, b \in \mathbb{R}^n$ be two initial conditions and $u^{[1]}, u^{[2]} \in PC([0,\infty],\mathbb{R}^m)$ be two input trajectories. Define the relative displacements as

$$\begin{gathered} \Delta y(t) = y_a^{[1]}(t) - y_b^{[2]}(t)\,,\; \Delta u(t) = u^{[1]}(t) - u^{[2]}(t)\,, \\ \Delta x(t) = x_a^{[1]}(t) - x_b^{[2]}(t)\,. \end{gathered} \tag{4}$$

[1] For instance, standard ResNet models whose hidden states evolve as $h_{k+1} = h_k + \Delta t\, f(h_k, \theta_k)$ can be interpreted as the ODE $\dot{h}(t) = f(h(t), \theta(t))$ as the discretization step Δt tends to zero.

Let

$$s_\Delta(\Delta u(t), \Delta y(t)) = \begin{bmatrix} \Delta y(t) \\ \Delta u(t) \end{bmatrix}^\top \begin{bmatrix} Q & S^\top \\ S & R \end{bmatrix} \begin{bmatrix} \Delta y(t) \\ \Delta u(t) \end{bmatrix}, \quad (5)$$

be a quadratic function $s_\Delta : \mathbb{R}^m \times \mathbb{R}^p \to \mathbb{R}$ parametrized by $Q \in \mathbb{R}^{p\times p}$, $S \in \mathbb{R}^{m\times p}$, $R \in \mathbb{R}^{m\times m}$. We recall the definition of dissipative systems that satisfy IQCs according to the supply rate (5).

Definition 2. A system Σ_θ in form (1) satisfies the *incremental* IQC defined by the matrices (Q, S, R), with $Q \preceq 0$ and $R = R^\top$, if there exists a function $\mathcal{S} : \mathbb{R}^n \to \mathbb{R}_0^+$ such that, for any two initial conditions $a, b \in \mathbb{R}^n$ and any two possible input functions $u^{[1]}, u^{[2]} \in PC([0,\infty], \mathbb{R}^m)$,

$$\mathcal{S}(\Delta x(t_1)) \leq \mathcal{S}(\Delta x(t_0)) + \int_{t_0}^{t_1} s_\Delta(\Delta u(t), \Delta y(t)) dt\,, \quad (6)$$

for every $t_1 \geq t_0$, where Δx, Δy and Δu are defined in (4) and the supply rate s_Δ is defined in (5).

If the function $\mathcal{S}(\Delta x(t))$ is continuous and differentiable, (6) can be rewritten as:

$$\frac{d}{dt}\Big(\mathcal{S}(\Delta x(t))\Big) \leq\ s_\Delta\big(\Delta u(t), \Delta y(t)\big)\,. \quad (7)$$

Despite being restricted to quadratic supply functions according to (5), IQCs can certify many incremental properties by appropriately selecting the values of (Q, S, R). It is worth noting that the assumptions in Definition 2

$$Q \preceq 0\,, \quad R = R^\top\,, \quad (8)$$

are fulfilled for several incremental properties of interest, see Table I.

Incremental Property	Q	R	S	$s_\Delta(\Delta u, \Delta y)$
L_2- gain bound ($\gamma \geq 0$)	$-\frac{1}{\gamma} I$	γI	0	$\gamma\lvert\Delta u\rvert^2 - \frac{1}{\gamma}\lvert\Delta y\rvert^2$
Passivity	0	0	$\frac{1}{2} I$	$\Delta u^\top \Delta y$
Input Passivity ($\nu \geq 0$)	0	$-2\nu I$	I	$\Delta u^\top \Delta y - \nu\lvert\Delta u\rvert^2$
Output Passivity ($\varepsilon \geq 0$)	$-2\varepsilon I$	0	I	$\Delta u^\top \Delta y - \varepsilon\lvert\Delta y\rvert^2$

TABLE I: Choices of (Q, S, R) to verify different incremental properties.

To summarize, our goal is to learn the parameters θ of a dynamical system (1) — i.e., a Neural ODE — that optimize a given cost as per (2), with the hard constraint that either (3) or (6) (or both) hold. This new requirement (i.e., the hard constraint) must be satisfied for all the parameters θ we optimize over. In other words, we consider a form of fail-safe learning, in the sense that the property of the model to be contracting or dissipative must be guaranteed during and after parameter optimization.

Remark 1. For solving problem (2), one has to select an integration scheme for (1), which allows performing forward propagation and gradient computations. The properties of the continuous-time model (1) may not coincide with those of the discretized one, in general. While in this paper our focus is on the contractivity and dissipativity properties of the continuous-time model (1), we remark that integration methods that preserve contractivity have been proposed in [21]. Tailoring these integration methods to IQC properties, or developing new ones, is an interesting direction for future work.

III. Contractivity and Dissipativity of NodeRENs

In this section, we present and analyze novel DNN structures that arise from appropriately combining Neural ODEs [10] with RENs [7]. The starting idea is to define the functions f_θ and g_θ in (1) through the model utilized for the layer equation in [7]. Specifically, we consider

$$\begin{bmatrix} \dot{x}(t) \\ v(t) \\ y(t) \end{bmatrix} = \overbrace{\begin{bmatrix} A & B_1 & B_2 \\ C_1 & D_{11} & D_{12} \\ C_2 & D_{21} & D_{22} \end{bmatrix}}^{\tilde{A}} \begin{bmatrix} x(t) \\ w(t) \\ u(t) \end{bmatrix} + \overbrace{\begin{bmatrix} b_x \\ b_v \\ b_y \end{bmatrix}}^{\tilde{b}}, \quad (9)$$

$$w(t) = \sigma(v(t)), \quad (10)$$

where $x(t) \in \mathbb{R}^n$, $u(t) \in \mathbb{R}^m$ and $y(t) \in \mathbb{R}^p$ are respectively the state, the input, and output at time t. The function $\sigma(\cdot)$ represents a nonlinear map and it is applied entry-wise. The input and output of $\sigma(\cdot)$ are $v(t), w(t) \in \mathbb{R}^q$, respectively. We denote system (9)-(10) as a NodeREN, and it can be interpreted as an affine time-invariant system in closed-loop with a static nonlinearity $\sigma(\cdot)$. In NodeRENs, the set of trainable parameters $\theta \in \mathbb{R}^{n_\theta}$ consists of the set $\tilde{A}$ of matrices (A, B_1, B_2, C_1, C_2, D_{11}, D_{12} and D_{22}) and the set $\tilde{b}$ of vectors (b_x, b_v, b_y) in (9).

The work [7] has established conditions that ensure contractivity and IQC properties of the *discrete-time* dynamics induced by θ. However, the same conditions on θ fail to ensure these properties for the continuous-time solutions of (9)-(10), in general.

Towards establishing contractivity and IQC-based dissipativity in continuous-time for the model (9)-(10), consider two different possible trajectories of the system, starting from two initial conditions a, $b \in \mathbb{R}^n$ and two input functions $u^{[1]}$, $u^{[2]} \in PC([0,\infty], \mathbb{R}^m)$. Then, define the *incremental form* of the system (9)-(10)

$$\begin{bmatrix} \Delta\dot{x}(t) \\ \Delta v(t) \\ \Delta y(t) \end{bmatrix} = \begin{bmatrix} A & B_1 & B_2 \\ C_1 & D_{11} & D_{12} \\ C_2 & D_{21} & D_{22} \end{bmatrix} \begin{bmatrix} \Delta x(t) \\ \Delta w(t) \\ \Delta u(t) \end{bmatrix}, \quad (11)$$

$$\Delta w(t) = \sigma(v_b^{[2]}(t) + \Delta v(t)) - \sigma(v_b^{[2]}(t))\,, \quad (12)$$

where Δx, Δy and Δu are defined in (4). Moreover, $\Delta v = v_a^{[1]}(t) - v_b^{[2]}(t)$, where $v_a^{[1]}$ and $v_b^{[2]}$ are the inputs of $\sigma(\cdot)$ for each trajectory. Next, we introduce two technical assumptions.

Assumption 1. The function $\sigma(\cdot)$ belongs to $PC([0,\infty], \mathbb{R})$ and its slope is restricted to the interval $[0, 1]$, that is

$$0 \leq \frac{\sigma(y) - \sigma(x)}{y - x} \leq 1\,, \quad \forall x, y \in \mathbb{R}\,, \quad x \neq y.$$

It is important to notice that, under Assumption 1, $\Delta v(t)$ and $\Delta w(t)$ verify the following inequality

$$\Gamma(t) = \begin{bmatrix} \Delta v(t) \\ \Delta w(t) \end{bmatrix}^\top \begin{bmatrix} 0 & \Lambda \\ \Lambda & -2\Lambda \end{bmatrix} [*] \geq 0, \quad \forall t \in \mathbb{R}, \quad (13)$$

for any diagonal matrix $\Lambda \succ 0$. Note that most of the popular activation functions used in the literature, such as the logistic function, $ReLU(\cdot)$ and $\tanh(\cdot)$, satisfy Assumption 1.

Assumption 2. The matrix D_{11} in (9) is strictly lower-triangular.

Assumption 2 enforces that each scalar entry of $\Delta v(t)$ only depends on the ones above it through (11). Hence, it becomes possibly to explicitly compute $\Delta v(t)$. This simplifies the numerical calculation of the solutions to (11)-(12), while guaranteeing that the model is very expressive thanks to the recursive application of the nonlinearity σ on successive entries of $\Delta v(t)$. The case where D_{11} is not lower-triangular is left for future work. We refer the interested reader to [7] for a discussion on implicit RENs in discrete-time.

In general, an ODE model may not admit a unique solution for a given initial condition and input trajectory [22]. We now proceed to show that (9)-(10) admits a unique solution for any choice of the parameters θ.

Lemma 1. Let Assumptions 1 and 2 hold. Then, the model (9)-(10) admits a unique solution in time for any $u(t) \in PC([0,\infty], \mathbb{R}^m)$, $x(0) \in \mathbb{R}^n$ and for any choice of the parameters $\theta \in \mathbb{R}^{n_\theta}$.

The proof, reported in Appendix A for completeness, is based on deriving a global Lipschitz constant by iterating through the nonlinearities defining the vector $v(t)$.

A. Characterization of Contracting and Dissipative NodeRENs

Here, we derive sufficient conditions over the parameters θ to guarantee contractivity and dissipativity of NodeRENs (9)-(10) according to a specified supply rate (5).

Theorem 1. A NodeREN (9)-(10) is contracting according to (3), if there exists a matrix $P \succ 0$ and a diagonal matrix $\Lambda \succ 0$ such that

$$\begin{bmatrix} -A^\top P - PA & -C_1^\top \Lambda - PB_1 \\ * & W \end{bmatrix} \succ 0, \quad (14)$$

with

$$W = 2\Lambda - \Lambda D_{11} - D_{11}^\top \Lambda. \quad (15)$$

Proof. Define

$$V_\Delta(t) = \Delta x(t)^\top P \Delta x(t), \quad (16)$$

and let

$$\Phi = (-A^\top P - PA) - (C_1^\top \Lambda + PB_1) W^{-1} (*)^\top \succ 0,$$

be the Schur complement of (14). Then, using properties of matrix inequalities, it is always possible to find an $\alpha \in (0, \lambda_{min}(\Phi)^{-1} \lambda_{max}(P)]$ such that $(\Phi - \alpha P) \succ 0$. Hence,

$$\begin{bmatrix} -A^\top P - PA - \alpha P & -C_1^\top \Lambda - PB_1 \\ * & W \end{bmatrix} \succ 0. \quad (17)$$

By left- and right-multiplying the inequality (17) with $\begin{bmatrix} \Delta x(t)^\top & \Delta w(t)^\top \end{bmatrix}$ and $\begin{bmatrix} \Delta x(t)^\top & \Delta w(t)^\top \end{bmatrix}^\top$, respectively, and using (13), we obtain by substitution that:

$$\dot{V}_\Delta(t) + \alpha V_\Delta(t) < -\Gamma(t) \leq 0.$$

Thus, according to Lyapunov's exponential stability theorem [23], the incremental system is globally exponentially stable, that is, it satisfies (3) with $c = \alpha/2$. □

For the rest of the paper, we refer to NodeRENs that comply with (14)-(15) as C-NodeRENs.

Remark 2. One may want to impose a certain convergence rate for a C-NodeREN. For this purpose, (14) can be modified as follows:

$$\begin{bmatrix} -A^\top P - PA - 2\tilde{\alpha} P & -C_1^\top \Lambda - PB_1 \\ * & W \end{bmatrix} \succ 0,$$

where the term $-2\tilde{\alpha}P$ enforces that (3) holds with $c = \tilde{\alpha}$. This can be directly seen by following the proof of Theorem 1 starting from (17).

Next, we characterize NodeRENs that comply with incremental IQCs.

Theorem 2. A NodeREN (9)-(10) satisfies the incremental IQC described by the triple (Q, S, R) fulfilling (8), if there exists a matrix $P \succ 0$ and a diagonal matrix $\Lambda \succ 0$ such that

$$\begin{bmatrix} -A^\top P - PA & -C_1^\top \Lambda - PB_1 & -PB_2 + C_2^\top S^\top \\ * & W & -\Lambda D_{12} + D_{21}^\top S^\top \\ * & * & \mathcal{R} \end{bmatrix} + \begin{bmatrix} C_2^\top \\ D_{21}^\top \\ D_{22}^\top \end{bmatrix} Q \begin{bmatrix} C_2^\top \\ D_{21}^\top \\ D_{22}^\top \end{bmatrix}^\top \succ 0, \quad (18)$$

with W given by (15) and

$$\mathcal{R} = R + SD_{22} + D_{22}^\top S^\top. \quad (19)$$

Proof. Consider the same function V_Δ as in (16). By left- and right-multiplying the inequality (18) with $\begin{bmatrix} \Delta x(t)^\top & \Delta w(t)^\top & \Delta u(t)^\top \end{bmatrix}$ and $\begin{bmatrix} \Delta x(t)^\top & \Delta w(t)^\top & \Delta u(t)^\top \end{bmatrix}^\top$ respectively, we obtain by substitution

$$\dot{V}_\Delta(t) - \begin{bmatrix} \Delta y(t) \\ \Delta u(t) \end{bmatrix}^\top \begin{bmatrix} Q & S^\top \\ S & R \end{bmatrix} [*] < -\Gamma(t) \leq 0.$$

Thus, the inequality (7) holds. □

For the rest of the paper, we refer to NodeRENs that comply with (18)-(19) as IQC-NodeRENs.

Remark 3. Note that all IQC-NodeRENs are also contracting for any choice of (Q, S, R) such that (8). Indeed, if there exists $P \succ 0$ and a diagonal matrix $\Lambda \succ 0$ such that (18) holds, then (14) also holds because $Q \preceq 0$ and the left-hand-side of (14) is a principal minor of that of (18).

It should be noted that solving the minimization problem (2) over C-NodeRENs or IQC-NodeRENs requires solving a semidefinite program (SDP) multiple times during the

optimization process. This can be computationally intractable for DNNs with several parameters. In the following section, we propose a parametrization of a rich class of C-NodeRENs and IQC-NodeRENs that circumevents this problem and allows for unconstrained optimization. It is worth noting that this approach is similar to [7] for discrete-time RENs, but the techniques differ due to the continuous-time nature of the proposed NodeRENs. Further, as we will show, our derivations do not introduce some sources of conservatism that are needed in the discrete-time case of [7].

B. Direct Parametrization of NodeRENs

Our goal is to define new free parameters $\theta_C \in \mathbb{R}^{n_C}$ and $\theta_{IQC} \in \mathbb{R}^{n_{IQC}}$ that can be mapped onto the parameters θ of the NodeREN model, given by equations (9)-(10), and such that either (14) or (18) are verified. First, we focus on constructing C-NodeRENs from the parameters $\theta_C \in \mathbb{R}^{n_C}$ given by

$$\theta_C = \{X, B_2, C_2, D_{12}, D_{21}, D_{22}, \tilde{b}, U, Y_1, X_P\}\,, \qquad (20)$$

where $X \in \mathbb{R}^{(n+q)\times(n+q)}$, $B_2 \in \mathbb{R}^{n\times m}$, $C_2 \in \mathbb{R}^{p\times n}$, $D_{12} \in \mathbb{R}^{q\times m}$, $D_{21} \in \mathbb{R}^{p\times q}$, $D_{22} \in \mathbb{R}^{p\times m}$, $\tilde{b} \in \mathbb{R}^{(n+q+p)}$ $U \in \mathbb{R}^{n\times q}$, $Y_1 \in \mathbb{R}^{n\times n}$ and $X_P \in \mathbb{R}^{n\times n}$.

Theorem 3. For any $\theta_C \in \mathbb{R}^{n_C}$ defined in (20), and $\epsilon, \epsilon_P > 0$ the two following statements hold.

1) There are matrices (Y, W, Z, P) of appropriate dimensions such that
$$\begin{bmatrix} -Y^\top - Y & -U - Z \\ * & W \end{bmatrix} = X^\top X + \epsilon I\,, \qquad (21)$$
$$P = X_P^\top X_P + \epsilon_P I\,. \qquad (22)$$
2) There are matrices $\{\tilde{A}, \tilde{b}\}$ defined in terms of θ_C and the matrices (Y, W, Z, P) defined in point 1, such that the corresponding NodeREN (9)-(10) is contracting.

Moreover, matrices (Y, W, Z, P) and $\{\tilde{A}, \tilde{b}\}$ can be computed as described in the proof of the Theorem.

Proof. Part 1): Define

$$H = \begin{bmatrix} H_{11} & H_{12} \\ H_{21} & H_{22} \end{bmatrix} = X^\top X + \epsilon I\,, \qquad (23)$$

where $H_{11} \in \mathbb{R}^{n\times n}$, $H_{12} \in \mathbb{R}^{n\times q}$, $H_{21} \in \mathbb{R}^{q\times n}$ and $H_{22} \in \mathbb{R}^{q\times q}$. Then, one can set

$$Y = -\frac{1}{2}(H_{11} + Y_1 - Y_1^\top)\,, \qquad (24)$$

and

$$W = H_{22}\,, \quad Z = -H_{12} - U\,. \qquad (25)$$

Thus, starting from H as in (23), (Y, W, Z) can be built using (24)-(25) and P using (22).

Part 2): First, note that $H \succ 0$ and $P \succ 0$ are guaranteed by construction because $X^\top X + \epsilon I$ and $X_P^\top X_P + \epsilon_P I$ are positive definite for any X and X_P. From Assumption 2, D_{11} is strictly lower triangular. Thus, using (15) and being $W = W^\top$ by construction, it is possible to split W as: $W = W_{diag} + W_{low} + W_{low}^\top$, where W_{diag} is a diagonal matrix, and W_{low} is a strictly lower triangular matrix. By setting

$$\Lambda = \frac{1}{2}W_{diag}\,, \quad D_{11} = -\Lambda^{-1}W_{low}\,, \qquad (26)$$

and the matrices A, B_1, C_1 can be retrieved as

$$C_1 = \Lambda^{-1}U^\top\,, \quad A = P^{-1}Y\,, \quad B_1 = P^{-1}Z\,, \qquad (27)$$

where P^{-1} and Λ^{-1} exist since $P \succ 0$ and $\Lambda \succ 0$. Finally, we can show that (14) holds by substituting A, B_1, C_1, D_{11}, Λ, and P with their definitions in (23)-(27). Thus, the corresponding NodeREN (9)-(10) specified by $\{\tilde{A}, \tilde{b}\}$ is contracting. □

In conclusion, an unconstrained parametrization of a class of C-NodeRENs is obtained by first freely choosing θ_C defined in (20), and then recovering the matrix $\tilde{A}$ using (24)-(27).

Remark 4. The equations (14) and (21) are equivalent for any $P \succ 0$, and (30) also holds for any $P \succ 0$. These aspects are different from [7, Theorem 1], where equivalence is not preserved due to the use of Young's inequality [24], and P must be designed jointly with the other parameters to satisfy contractivity and dissipativity. This improved generality can have a favorable impact on solving (2) when searching in the set of C-NodeRENs.

Next, we focus on NodeRENs that satisfy IQC constraints by design, i.e. for any choice of parameters $\theta_{IQC} \in \mathbb{R}^{n_{IQC}}$ given by

$$\theta_{IQC} = \{X_R, B_2, C_2, D_{21}, \tilde{b}, X_3, T, U, Y_1, X_P\}\,, \qquad (28)$$

where $X_R \in \mathbb{R}^{(n+q)\times(n+q)}$, $B_2 \in \mathbb{R}^{n\times m}$, $C_2 \in \mathbb{R}^{p\times n}$, $D_{21} \in \mathbb{R}^{p\times q}$, $\tilde{b} \in \mathbb{R}^{(n+p+q)}$, $X_3 \in \mathbb{R}^{s\times s}$, $T \in \mathbb{R}^{q\times m}$, $U \in \mathbb{R}^{n\times q}$, $Y_1 \in \mathbb{R}^{n\times n}$ and $X_P \in \mathbb{R}^{n\times n}$. In the next theorem, we provide a procedure to construct an IQC-NodeREN for any choice of θ_{IQC}.

Theorem 4. Let (Q, S, R) be such that (8). Assume also that there exists $\delta > 0$ satisfying $R - S(Q - \delta I)^{-1}S^\top \succ 0$. For any $\theta_{IQC} \in \mathbb{R}^{n_{IQC}}$ defined in (28), and $\epsilon, \epsilon_P > 0$ the two following statements hold.

1) There are matrices (Y, W, Z, P, D_{22}) of appropriate dimensions such that
$$\tilde{\mathcal{R}} = R + SD_{22} + D_{22}^\top S^\top + D_{22}^\top Q D_{22} \succ 0\,, \qquad (29)$$
$$\begin{bmatrix} -Y^\top - Y & -U - Z \\ * & W \end{bmatrix} - \Psi = X_R^\top X_R + \epsilon I\,, \qquad (30)$$
where P is constructed as in (22), and
$$\Psi = \begin{bmatrix} V \\ \tilde{T} \end{bmatrix} \tilde{\mathcal{R}}^{-1} \begin{bmatrix} * \end{bmatrix}^\top - \begin{bmatrix} C_2^\top \\ D_{21}^\top \end{bmatrix} Q \begin{bmatrix} * \end{bmatrix}^\top\,, \qquad (31)$$
$$\tilde{T} = -T + D_{21}^\top S^\top + D_{21}^\top Q D_{22}\,, \qquad (32)$$
$$V = -PB_2 + C_2^\top S^\top + C_2^\top Q D_{22}\,. \qquad (33)$$
2) There are matrices $\{\tilde{A}, \tilde{b}\}$ defined in terms of θ_{IQC} and the matrices (Y, Z, W, P, D_{22}) defined in point 1, such

that the corresponding NodeREN (9)-(10) satisfies the incremental IQCs parametrized by (Q, S, R).

The proof of Theorem 4 shares similarities with the one of Proposition 2 in [7] and it is reported in Appendix B. Note that the assumption that there exists a δ such that $R - S(Q - \delta I)^{-1}S^\top \succ 0$ is not restrictive. Indeed, for all the most relevant cases, reported in Table I, finding an appropriate value of δ is straightforward. In conclusion, an unconstrained parametrization of IQC-NodeRENs is obtained by first freely choosing the parameters $\theta_{IQC} \in \mathbb{R}^{n_{IQC}}$, then constructing D_{22} as per (40) in Appendix B, and last recovering the matrices $\tilde{A}$ using (24)-(27), (40) and (41).

IV. Simulations & Results

In this section, we demonstrate the use of NodeRENs for the identification of a stable nonlinear system. First, we evaluate the performance of NodeRENs through different integration methods during the training phase — not possible in discrete-time systems. Second, we illustrate the benefits of contractivity-by-design by training a general non-contractive NodeREN (11)-(12), which fails to learn a stable behavior for the same task. Last, we show the ability of NodeRENs to learn from data that are not sampled regularly in time, while maintaining the guarantees by design. The code used in this work is available at `https://github.com/DecodEPFL/NodeREN`.

We remark that the trajectories of NodeRENs are reversible in time due to Lemma 1, and hence they cannot intersect for different initial conditions. To increase the expressivity of the model, in the simulations we use augmented state vectors and initialize to zero the additional scalar states. This technique, also known as feature augmentation, has been proposed in [25] for general Neural ODEs.

A. Continuous-Time System Identification

Here, we consider the system identification of a black-box system. For this experiment, we assume that the unknown system dynamics are those of a nonlinear pendulum

$$\ell\ddot{\alpha}(t) + \beta\dot{\alpha}(t) + g\sin\alpha(t) = 0\,, \tag{34}$$

where $\alpha(t)$ is the angle position of the pendulum at time t with respect to the vertical axis, $\beta > 0$ is the viscous damping coefficient, g is the gravitational acceleration and $\ell > 0$ is the length of the pendulum. The available measurements are given by $z(t) = [\alpha(t)\ \ \dot{\alpha}]^\top + w^\top(t)$, where $w(t) \in \mathbb{R}^2$ denotes measurement noise. We assume $w(t)$ to be Gaussian noise.

We consider the scenario where the system dynamics to identify are unknown and the only prior knowledge we have is that system is stable around the origin. Hence, we choose to train a C-NodeREN, which is guaranteed to be contracting (and so, stable around the origin if $\tilde{b}$ is null) for any choice of the trainable parameters θ_C — i.e. even if we stop the optimization prematurely. Specifically, we minimize the mean squared error (MSE) function

$$\min_{\theta_C} \quad \frac{1}{N}\sum_{i=1}^{N}\frac{1}{n_i}\sum_{j=1}^{n_i}|z^i_{\theta_C}(t^i_j) - \tilde{z}^i(t^i_j)|^2\,, \tag{35}$$

using minibatch gradient descent with Adam optimizer [26]. In (35), $\tilde{z}^i$ represents a collection of vectors in $\mathbb{R}^2$ defined as $\tilde{z}^i = \{z(t^i_j), \forall t^i_j \in \mathcal{T}^i\}_{i=0}^N$, where $\mathcal{T}^i$ is the set of n_i time instants where the target system is sampled, and N is the total number of experiments in the training data-set. Similarly, $z^i_{\theta_C}$ is the collection of outputs of the C-NodeREN at each time instant in the set $\mathcal{T}^i$. To evaluate the loss in (35), we select a batch of η initial conditions for both the pendulum and the C-NodeREN. We then simulate the free evolution of both dynamical systems up to time T_{end} (using a chosen integration method) and compare the values of the trajectories at the desired time instants in the set $\mathcal{T}^i \subset [0, T_{end}]$. Finally, we consider N_{test} new experiments to test the model and we evaluate the prediction performance by comparing the true system and the learned model in a longer time window, i.e. at some instants $\mathcal{T}^i_{test} \subset [0, T^{test}_{end}]$, for $T^{test}_{end} > T_{end}$.

The chosen C-NodeREN architecture has $n = 4$ and $q = 5$. It comes with $\theta_C \in \mathbb{R}^{\sim 150}$, and it is trained using the following integration methods: forward Euler (`euler`), Runge-Kutta of order 4 (`rk4`), and Dormand-Prince-Shampine of order 5 (`dopri5`). We train each model for 30 epochs, with a batch size $\eta = 20$, a training data-set of $N = 200$ experiments, and a testing data-set of $N_{test} = 200$ experiments. We consider measurement noise with Gaussian distribution with zero mean and 0.01 standard deviation. We set $T_{end} = 2s$ and $T^{test}_{end} = 8s$. For each experiment i of the training (test) data-set, we collect $n_i = 45$ ($n^{test}_i = 180$), datapoints of the trajectory which are randomly sampled in the time interval $[0, T_{end}]$ ($[0, T^{test}_{end}]$). In Figure 1, we report the resulting test losses for different methods, along with their number of function evaluations (NFE) used for the prediction in the time window $[0, T^{test}_{end}]$. Both `euler` and `rk4` have been applied using 120 and 200 integration steps in $[0, T^{test}_{end}]$. One of the advantages of variable-steps methods such as `dopri5` is the possibility to choose a tolerance value *tol* to fix the computational error during the ODE simulation. Indeed, it is possible to obtain a trade-off between accuracy and the required number of function evaluations just by setting properly this parameter. It is important to emphasize how for fixed-step methods (e.g., `euler`, `rk4`) the chosen number of steps may not be enough to properly capture the dynamics of the trained model. This can lead to numerical instability. Instead, adaptive methods (e.g., `dopri5`) can *adapt* the integration step on the fly, keeping the integration error bounded. As anticipated in Remark 1, it is of future work to endow C-NodeRENs with specific integration methods that preserve contractivity, e.g. [21].

Then, for the same identification task, we have trained a general NodeREN (11)-(12) (that we denote as G-NodeREN in what follows for brevity), with trainable parameters $\theta = \{\tilde{A}, \tilde{b}\}$. Given the higher flexibility of the model in (11)-

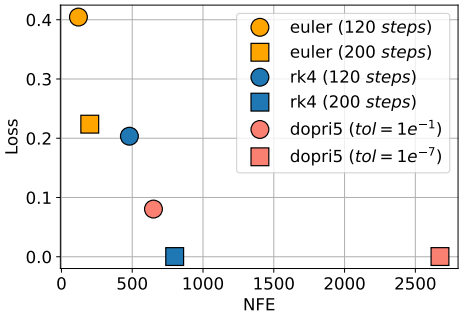

Fig. 1: Comparison between the number of function evaluations (NFE) and loss on testing data-set for different integration methods.

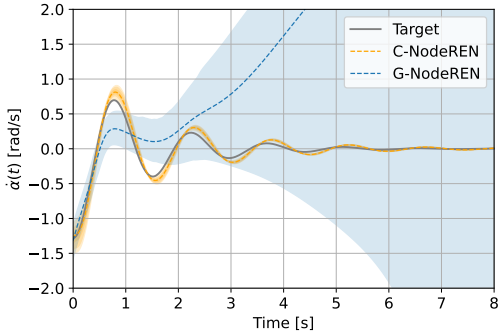

Fig. 2: Target angular velocity of the pendulum (gray) and test trajectories of a C-NodeREN (orange) and a G-NodeREN (blue). Confidence intervals of 50%, 80% and 95% —indicated in shade— show the distribution of the trajectories when adding a perturbation to the initial condition of the considered model.

(12) with respect to C-NodeRENs, one could expect a better performance after training. However, a given choice of parameters θ in (11)-(12) can lead to unstable dynamics; see for instance Figure 2. When this happens, the model incurs large losses, from which it may be difficult (or impossible) to recover to a stable model by gradient descent. Instead, C-NodeRENs limit the search to stable models only, resulting in better identification performance for the considered example. Figure 2 also show the 50%, 80% and 95% confidence intervals when adding perturbations on the initial conditions of the trained models. By initializing the models on $z(0)+d$ with d representing Gaussian noise with a standard deviation of 0.1. As expected, the C-NodeREN trajectories converge to each other while this is not the case for the G-NodeREN ones.

B. Irregularly sampled-data

The data acquired during experiments may suffer from time delays and thus be sampled inconsistently, making the application of discrete-time systems difficult. Instead, NodeRENs can handle irregularly sampled-data, thanks to their continuous-time nature. In order to show the robustness of C-NodeRENs with respect to the irregularly sample data, we compare the test losses of 10 C-NodeRENs trained over 10 different training data-sets having the same initial conditions, but different sampling times. We observe that, despite using differently sampled data, all the models have similar test losses: they all laid in the interval $[3.7 \times 10^{-4}; 9.1 \times 10^{-3}]$, depending on how well the samples were distributed.

V. Conclusions

In this work, we have established a class of Neural ODEs that generalize RENs for continuous-time scenarios. Specifically, the proposed models guarantee relevant continuous-time system-theoretic properties such as contractivity and dissipativity by design. The resulting DNNs can be trained using unconstrained optimization — which enables the use of large networks — and the resulting architectures are flexible in the choice of an ODE integration scheme that is suitable for the learning problem at hand. We have showcased performance of our NodeRENs through the identification of a nonlinear pendulum, where the data are measured at irregularly spaced time instants.

An important direction for future research is to develop integration schemes that provably preserve contractivity and IQC properties for NodeRENs. It is also relevant to study distributed NodeREN architectures, and to characterize their generalization properties.

References

[1] I. H. Sarker, "Machine learning: Algorithms, real-world applications and research directions," *SN computer science*, vol. 2, no. 3, p. 160, 2021.

[2] C. Szegedy, W. Zaremba, I. Sutskever, J. Bruna, D. Erhan, I. Goodfellow, and R. Fergus, "Intriguing properties of neural networks," *International Conference on Learning Representations*, 2014.

[3] M. Cheng, J. Yi, P.-Y. Chen, H. Zhang, and C.-J. Hsieh, "Seq2Sick: Evaluating the robustness of sequence-to-sequence models with adversarial examples," *Proceedings of the AAAI Conference on Artificial Intelligence*, vol. 34, pp. 3601–3608, Apr. 2020.

[4] E. Haber and L. Ruthotto, "Stable architectures for deep neural networks," *Inverse Problems*, vol. 34, p. 014004, dec 2017.

[5] M. Zakwan, L. Xu, and G. Ferrari-Trecate, "Robust classification using contractive Hamiltonian neural ODEs," *IEEE Control Systems Letters*, vol. 7, pp. 145–150, 2023.

[6] K.-K. K. Kim, E. R. Patrón, and R. D. Braatz, "Standard representation and unified stability analysis for dynamic artificial neural network models," *Neural Networks*, vol. 98, pp. 251–262, 2018.

[7] M. Revay, R. Wang, and I. R. Manchester, "Recurrent Equilibrium Networks: Flexible Dynamic Models with Guaranteed Stability and Robustness," *arXiv preprint arXiv:2104.05942*, 2021.

[8] R. Wang and I. R. Manchester, "Youla-REN: Learning nonlinear feedback policies with robust stability guarantees," *2022 American Control Conference (ACC)*, pp. 2116–2123, 2021.

[9] K. J. Åström, P. Hagander, and J. Sternby, "Zeros of sampled systems," *Automatica*, vol. 20, no. 1, pp. 31–38, 1984.

[10] R. T. Q. Chen, Y. Rubanova, J. Bettencourt, and D. Duvenaud, "Neural ordinary differential equations," *Advances in Neural Information Processing Systems*, 2018.

[11] L. S. Pontryagin, *The mathematical theory of optimal processes*. CRC press, 1987.

[12] P. Kidger, J. Morrill, J. Foster, and T. Lyons, "Neural controlled differential equations for irregular time series," *Advances in Neural Information Processing Systems*, vol. 33, pp. 6696–6707, 2020.

[13] C. L. Galimberti, L. Furieri, L. Xu, and G. Ferrari-Trecate, "Hamiltonian deep neural networks guaranteeing non-vanishing gradients by design," *IEEE Transactions on Automatic Control*, 2023.

[14] S. Massaroli, M. Poli, M. Bin, J. Park, A. Yamashita, and H. Asama, "Stable neural flows," *arXiv preprint arXiv:2003.08063*, 2020.
[15] D. Martinelli, C. Galimberti, I. R. Manchester, L. Furieri, and G. Ferrari-Trecate, "Direct optimization of contracting and robust deep neural networks in continuous time," *arXiv preprint arXiv:????.????*, 2023.
[16] K. He, X. Zhang, S. Ren, and J. Sun, "Deep residual learning for image recognition," in *Proceedings of the IEEE conference on computer vision and pattern recognition*, pp. 770–778, 2016.
[17] E. Hairer, G. Wanner, and S. P. Nørsett, *Solving Ordinary Differential Equations I*. Springer Berlin Heidelberg, 1993.
[18] Q. Kang, Y. Song, Q. Ding, and W. P. Tay, "Stable neural ODE with Lyapunov-stable equilibrium points for defending against adversarial attacks," *Advances in Neural Information Processing Systems*, vol. 34, pp. 14925–14937, 2021.
[19] A. Van der Schaft, *L2-gain and passivity techniques in nonlinear control*. Springer, 2000.
[20] P. Pauli, A. Koch, J. Berberich, P. Kohler, and F. Allgöwer, "Training robust neural networks using Lipschitz bounds," *IEEE Control Systems Letters*, vol. 6, pp. 121–126, 2021.
[21] I. R. Manchester, "Contracting nonlinear observers: Convex optimization and learning from data," in *2018 Annual American Control Conference (ACC)*, pp. 1873–1880, 2018.
[22] J. Lygeros and F. Ramponi, "Lecture notes on linear system theory," *Automatic Control Laboratory, ETH Zurich*, 2015.
[23] H. K. Khalil, *Nonlinear systems; 3rd ed.* Upper Saddle River, NJ: Prentice-Hall, 2002.
[24] A. Zemouche, R. Rajamani, B. Boulkroune, H. Rafaralahy, and M. Zasadzinski, "H-inf circle criterion observer design for Lipschitz nonlinear systems with enhanced LMI conditions," in *2016 American Control Conference (ACC)*, pp. 131–136, 2016.
[25] E. Dupont, A. Doucet, and Y. W. Teh, "Augmented neural ODEs," *Advances in neural information processing systems*, vol. 32, 2019.
[26] S. Ruder, "An overview of gradient descent optimization algorithms," *arXiv preprint arXiv:1609.04747*, 2017.

APPENDIX

A. Proof of Lemma 1

Given $u(t) \in PC([0,\infty], \mathbb{R}^m)$, we can rewrite (9) as:

$$\dot{x}(t) = p(x(t),t) = Ax(t) + B_1 w(t) + B_2 u(t) + b_x, \quad (36)$$

where we define $p(x(t),t) = f(x(t),u(t),t)$. It is well-known that a solution exists and is unique if $p(\cdot,\cdot)$ is globally Lipschitz in its first argument and piece-wise continuous in its second (e.g., [22, Theorem 3.6]). Hence, we prove that these properties hold for the model in (9) under Assumptions 1 and 2. First, $p(\cdot,\cdot)$ is piece-wise continuous in its second argument because it is the composition of piece-wise continuous functions under Assumption 1. Then, we prove that $p(\cdot,\cdot)$ is globally Lipschitz in its first variable, that is

$$\exists \kappa > 0 : |p(x_1,t) - p(x_2,t)| \leq \kappa |x_1 - x_2|,$$

for every $x_1, x_2 \in \mathbb{R}^n$ and $t \in \mathbb{R}$. For $j \in \{1,2\}$, denote $w_j \in \mathbb{R}^q$ as

$$w_j = \begin{bmatrix} w_j^1 \\ \vdots \\ w_j^q \end{bmatrix} = \sigma(v_j) = \begin{bmatrix} \sigma(v_j^1) \\ \vdots \\ \sigma(v_j^q) \end{bmatrix},$$

where $v_j = C_1 x_j + D_{11} w_j + D_{12}\hat{u}$ for any possible value $\hat{u}$ of the function $u(t)$ in time. We have

$$|p(x_1,t) - p(x_2,t)| = |A(x_1 - x_2) + B_1(w_1 - w_2)|,$$

Using the triangle inequality, we have

$$|p(x_1,t) - p(x_2,t)| \leq |A|\,|x_1 - x_2| + |B_1|\,|w_1 - w_2|. \quad (37)$$

Using Assumption 1 and Assumption 2 we verify

$$|w_1^1 - w_2^1| \leq |C_1^{1:}||x_1 - x_2|,$$

where $C_1^{i:}$ denotes the i^{th} row of C_1, and we define $\kappa_1 = |C_1^{1:}|$. Proceeding similarly for each entry of $w_1 - w_2$ we derive

$$|w_1^2 - w_2^2| \leq \kappa_2 |x_1 - x_2|,$$
$$\vdots$$
$$|w_1^q - w_2^q| \leq \kappa_q |x_1 - x_2|,$$

with Lipschitz constants $\{\kappa_2, \dots \kappa_q\}$ obtained as $\kappa_i = |C_1^{i:}| + \sum_{\ell=1}^{i-1} |D_{11}^{i,\ell}| \kappa_\ell$ for $i = 2, \dots, q$, where $D_{11}^{i,j}$ denotes the element in the i^{th} row and j^{th} column of D_{11}. Finally, from (37) we conclude $|p(x_1,t) - p(x_2,t)| \leq \kappa_{tot} |x_1 - x_2|$, where $\kappa_{tot} = |A| + \sum_{i=1}^{q} |B_1^{i:}| \kappa_i$. Thus, the differential equation $\dot{x}(t) = f(x(t),u(t),t) = p(x(t),t)$ is globally Lipschitz in x with constant $\kappa_{tot} \in \mathbb{R}_0^+$ and its solution exists and it is unique.

B. Proof of Theorem 4

We first need a technical lemma.

Lemma 2. Let $p, m \in \mathbb{N}$, and $s = \max(p,m)$. Let $M \in \mathbb{R}^{s \times s}$, and $M = M^\top \succ 0$. Define

$$F = (I - M)(I + M)^{-1}, \quad (38)$$

and $\tilde{F} = [F]_{p \times m}$. Then it follows that $I - \tilde{F}^\top \tilde{F} \succ 0$.

The proof is reported in our Technical Note [15]. Note that the property (38) has also been used in [7]. In this work, we have derived a full proof for completeness. We are now ready to present the proof of Theorem 4.

Proof. Part 1): Define $\mathcal{Q} = Q - \delta I$. Since $\mathcal{Q} \prec 0$ and $R - S(Q - \delta I)^{-1} S^\top \succ 0$, there exist $L_Q \succ 0$ and $L_R \succ 0$ with

$$L_Q^\top L_Q = -\mathcal{Q}, \quad L_R^\top L_R = R - S\mathcal{Q}^{-1} S^\top. \quad (39)$$

Next, define $M = X_3^\top X_3 + \epsilon I$ and $\tilde{F} = \left[(I - M)(I + M)^{-1}\right]_{p \times m}$. Construct D_{22} as

$$D_{22} = -\mathcal{Q}^{-1} S^\top + L_Q^{-1} \tilde{F} L_R. \quad (40)$$

We now show that this choice of D_{22} leads to $\tilde{\mathcal{R}} \succ 0$. Let $\Phi = R + SD_{22} + D_{22}^\top S^\top + D_{22}^\top \mathcal{Q} D_{22}$. Since $\tilde{\mathcal{R}} = \Phi + \delta D_{22}^\top D_{22}$, it suffices to prove that $\Phi \succ 0$. After plugging (40) in the definition of Φ, we obtain $\Phi = L_R^\top (I - \tilde{F}^\top \tilde{F}) L_R$ by cancellation of addends and by using (39). By Lemma 2 and since $L_R \succ 0$, we conclude that $\Phi \succ 0$.

Finally, we indicate how to construct (Y, W, Z) such that (30) holds. Compute Ψ from (31) and define

$$H = \begin{bmatrix} H_{11} & H_{12} \\ H_{21} & H_{22} \end{bmatrix} = X_R^\top X_R + \epsilon I + \Psi.$$

Then, using H, it is possible to use the same steps of Theorem 3 to compute (Y, W, Z) from (24)-(25), and P from (22). This choice satisfies the equality (30) by construction.

Part 2): We show how to parametrize the matrices in $\tilde{A}$. First, note that $P \succ 0$ holds due to (22). Construct Λ and D_{11} using (26), and define the matrices (A, B_1, C_1, D_{11}) as per (27). Set

$$D_{12} = \Lambda^{-1} T. \tag{41}$$

Then, when choosing the parameters according to part 1 of this Theorem and plugging in the matrices just defined, Ψ satisfies $\Psi = \Psi^\top \succeq 0$ since $\tilde{\mathcal{R}} \succ 0$ and $Q \preceq 0$. Moreover, $H - \Psi = X_R^\top X_R + \epsilon I \succ 0$. Thus, $H = H^\top \succ 0$, and it holds that $W = W^\top \succ 0$ and $\Lambda \succ 0$. Thus, the NodeREN defined by $\{\tilde{A}, \tilde{b}\}$ complies with (18), and thus it satisfies the incremental IQCs parametrized by (Q, S, R). □